ISBN: 978-3-95450-231-8 ISSN: 2673-5490 doi: 10.18429/JACoW-IPAC2023-MOPA090

LATTICE AND DETECTOR STUDIES FOR THE MDI OF A 10 TEV MUON COLLIDER

D. Calzolari, C. Carli, A. Lechner, D. Schulte, K. Skoufaris, CERN, Geneva, Switzerland
D. Lucchesi, INFN Padova, Italy, N. Bartosik, N. Pastrone, INFN Torino, Italy
F. Collamati, INFN Roma, Italy

Abstract

Among the possible future lepton colliders under study, circular muon colliders have the largest potential of reaching center-of-mass energies of 10+ TeV. Being more massive than electrons and positrons, muons are much less affected by synchrotron radiation emission, but they suffer from the drawback of having a limited lifetime. As a consequence of their decay, intense secondary radiation fields are generated in the collider, which can considerably disrupt the detector performance, both as physics background and as a cause of long-term material degradation. Therefore, the machine-detector interface in a muon collider requires a careful design, integrating massive shielding elements between the detector and final focus magnets. In this paper, we devise an interaction region design for a 10 TeV muon collider with a final focus triplet. We quantify the flux of secondary particles entering the detector by means of shower simulations and provide a first optimization of the shielding configuration.

INTRODUCTION

Future discovery machines for high-energy physics require unprecedented centre-of-mass energies and luminosities. Circular electron-positron colliders are strongly limitated by synchrotron radiation (SR) emission, while linear electron colliders, like ILC [1] and CLIC [2], require very long accelerating sections. The possible energy reach in hadron colliders [3] is much higher than in electron-positron machines, but only a fraction of the centre-of-mass energy is available in the collisions due to the composite structure of the proton (a bound state of quarks and gluons). Muon colliders [4, 5] offer the benefit of both categories: they collide fundamental particles, without being limited by SR emission due to a mass 200 times larger than the $e^{-/+}$ one.

However, muons have an unstable nature, with a rest lifetime of 2.2 μs. As muons decay product, neutrinos travel through the machine unperturbed, while the decay $e^{-/+}$ generate intense electromagnetic showers and give rise to secondary neutrons, mainly due to photo-nuclear interactions. In the proximity of the collider experimental interaction point (IP), these secondaries can travel inside the detector area and can impede the physics performance and cause radiation damage in detector components. To mitigate this phenomenon, past studies [6, 7] within the Muon Accelerator Program (MAP) [8] suggested the use of thick conical shielding elements between the last final focus magnet and the detector. These so-called nozzles aim at reducing the beam-induced background (BIB) by several orders of magnitude. The nozzles are assumed to be made of tungsten, with an outer layer of borated polyethylene for reducing the neutron flux. While the MAP studies focused on collider energies ranging from $\sqrt{s}$ = 125 GeV (Higgs factory) up to a few TeV, the recently formed International Muon Collider Collaboration is studying a higher-energy collider with $\sqrt{s} \geq 10$ TeV [9].

In this paper, we discuss the interaction region (IR) design for a 10 TeV collider and present BIB studies with FLUKA [10–12]. As a starting point, we consider the existing MAP nozzle optimized for $\sqrt{s} = 1.5$ TeV (see Fig. 1). The magnetic lattice has been designed from scratch [13]. First results of our background studies have been presented in [14], illustrating the effect of dipolar components in the final focus region. The dipole fields reduce the contribution of distant decays, but the overall benefit was found to be limited since the background is dominated by decays in final focus magnets. In this paper, we assess the dependency on L^* and present first optimization studies for the nozzle tip. In the second half of the paper, we provide a first assessment of the radiation damage in the 10 TeV detector.

LATTICE AND NOZZLE

Beam-Induced Background Versus L^*

The baseline IR lattice configuration for the 10 TeV collider assumes the distance between the interaction point and the last magnet $L^* = 6$ m, with betatron function in the interaction point β^*=1.5 mm and a maximum allowed magnetic field of 20 T at the magnet aperture (see Fig. 2) [13]. In the detector region, we consider a uniform solenoidal field of 5 T. The first 10 TeV studies [14] showed that muons decaying in the nozzle area do not contribute significantly

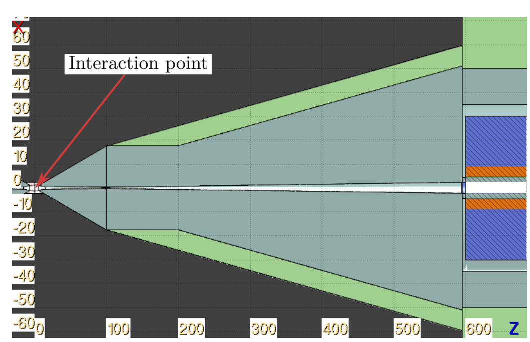

Figure 1: Nozzle between IP and first quadrupole as implemented in FLUKA. Only the right nozzle is shown. Both axes are expressed in cm.

ISBN: 978-3-95450-231-8 ISSN: 2673-5490 doi: 10.18429/JACoW-IPAC2023-MOPA090

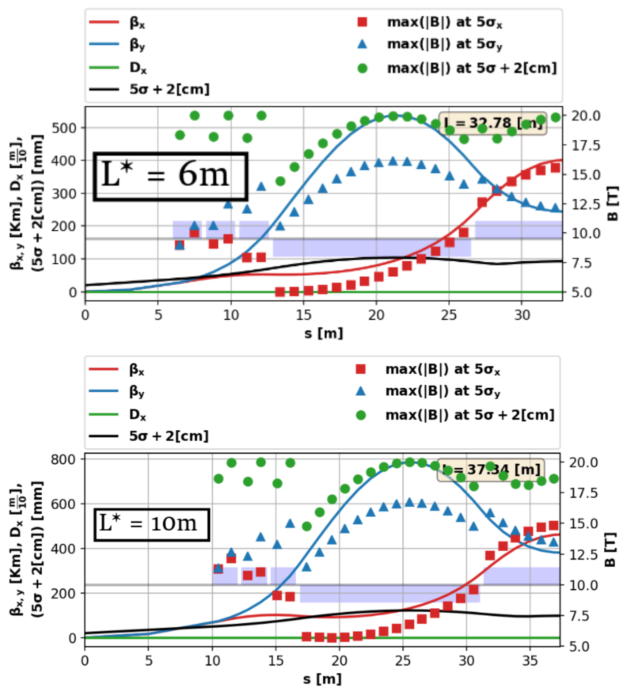

Figure 2: Final focus lattice for a $\sqrt{s}$ = 10 TeV muon collider. Top: baseline with L^* = 6 m, bottom: alternative lattice with L^* = 10 m.

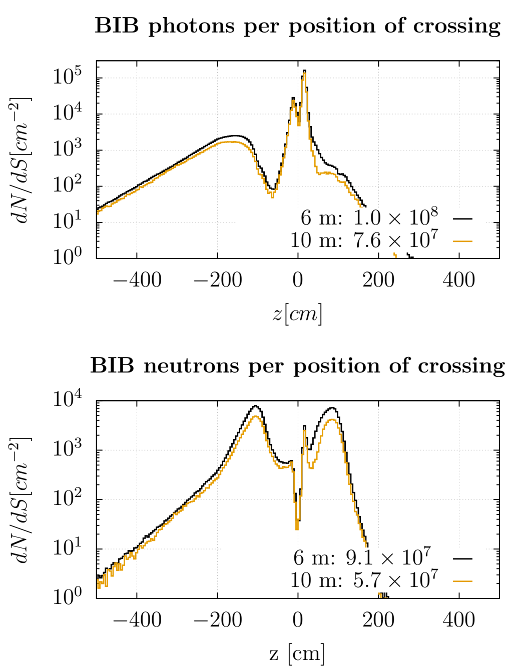

Figure 3: The number of photons (top) and neutrons (bottom) entering the detector volume per unit surface (per bunch crossing). A larger L^* of 10 m leads to a moderate reduction of the BIB compared to L^* = 6 m. Only the contribution of the μ^+ bunch is shown (beam direction is from the left to the right).

to the BIB. The strong solenoid field traps the $e^{-/+}$, which travel in the beam vacuum until they reach the other side of the interaction region, depositing their energy in the machine components. As shown in [14], muon decays within $|z| < L^*$ contribute several orders of magnitudes less to the BIB than those in final focus quadrupoles.

In order to assess the impact of L^* on the BIB, an alternative lattice with L^* = 10 m was devised (see Fig. 2). The peak magnetic field at the quadrupole aperture and β^* was assumed to be same as for L^* = 6 m. The longer L^* requires larger β-functions in the magnets, therefore increasing the magnet aperture. On the other hand, the quadrupole gradient is smaller due to the 20 T limitation and the increased aperture, thus implying a longer final focus scheme. To compare the background for both lattices, we consider a single μ^+ bunch circulating in clockwise direction, with a bunch intensity of 1.8×10^{12} muons. The transport cut for secondary particles was assumed to be 100 keV, except for neutrons, which were transported down to 10^{-5} eV.

Figure 3 shows the number of photons and neutrons per unit surface entering the detector in proximity of the IP ($|z| < 5$ m); results are given per bunch crossing. The longitudinal distribution has a similar shape for both lattice configurations, since the profiles are dominated by the nozzle shape. The total number of particles is similar in both cases, with a reduction of around 20% for photons and 40% for neutrons in the L^* = 10 m layout. Electrons and positrons, which are less abundant than photons and neutrons, exhibit a similar decrease as the photon component. Considering the higher complexity of the L^* = 10 m layout, the obtained reduction is not considered significant enough for increasing L^* to 10 m.

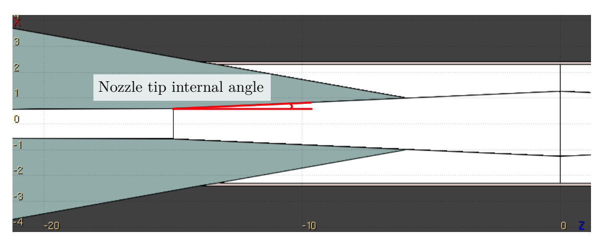

Figure 4: Zoom on the nozzle tip up to 20 cm from the IP. The angle under consideration is highlighted. Both axes are expressed in cm.

Nozzle Tip

The tip of the nozzle plays a significant role for the background in the proximity of the IP. While first attempts to optimize the outer nozzle shape for 10 TeV were shown in [14], we present here first background studies for different nozzle tip configurations. Several simulations were performed, varying the internal angle of the nozzle tip as shown in Fig. 4. All other geometrical features of the nozzle were kept the same. Figure 5 reports the obtained distributions of photons and neutrons entering the detector around the IP. Like above, only the contribution of the μ^+ bunch is shown. Compared to the angle of 2.5 deg used for the MAP nozzle, we observe a

ISBN: 978-3-95450-231-8 ISSN: 2673-5490 doi: 10.18429/JACoW-IPAC2023-MOPA090

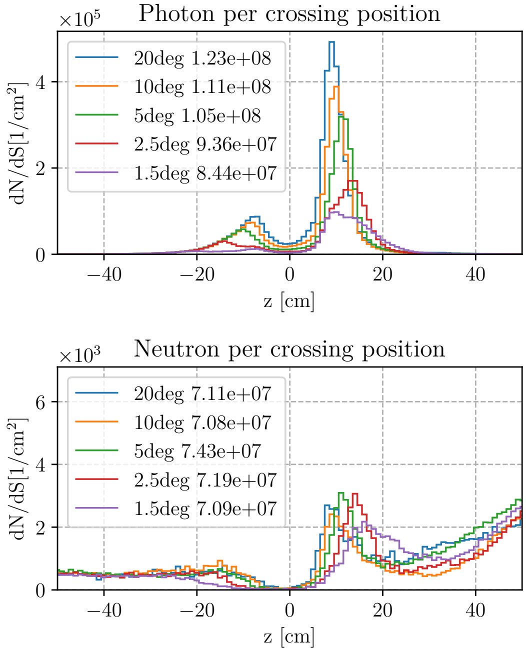

Figure 5: Photons (top) and neutrons (bottom) entering the detector volume per unit surface (per bunch crossing). The different curves correspond to different internal angles of the nozzle tip; the baseline angle is 2.5 deg. Changing it to 1.5 deg can reduce the peak in the photon fluence profile. The same reduction applies to electrons and positrons, while neutrons are mostly unaffected.

reduction of the peak fluence when reducing the angle, while increasing the angle degrades the background. These results highlights the potential of reducing the particle fluence into the inner tracker by optimizing the shielding configuration. More studies are needed to optimize the entire nozzle shape for 10 TeV.

DETECTOR RADIATION DAMAGE

A first evaluation of the cumulative radiation damage in the detector of a 1.5 TeV muon collider has been presented in [15]. By design, the decay-induced power loss per meter is the same as in the 10 TeV collider (about 500 W/m) due to a smaller circumference of the 1.5 TeV ring. The 1 MeV-neutron equivalent fluence for one year of operation was found to reach $\Phi_{n_{eq}} = 1 \times 10^{15}\,\mathrm{cm}^{-2}$ in the inner tracker of the 1.5 TeV detector [15], which is comparable to HL-LHC [16].

In this paper, assuming a a MAP-like nozzle, we present a first estimate of the muon decay-induced radiation damage in the detector of a 10 TeV muon collider with $L^* = 6\,\mathrm{m}$. To normalize the results, we assume that the beam is not extracted and fully decays in the 10 km collider ring. We further assume that bunches are injected with a repetition rate of 5 Hz, considering 200 days of operation per year. This is a conservative assumption, since the design parameters indicate that the design integrated luminosity can be reached in a shorter operation time. With a two-step simulation approach, the BIB particles obtained in the machine simulation were propagated in a simplified detector model. Figure 6 presents the 1 MeV-neutron equivalent fluence map for one year of operation. Only the contribution of one beam is shown. The results indicate similar $\Phi_{n_{eq}}$ values in the inner tracker as for the 1.5 TeV collider. This is a promising observation, indicating that the different decay spectrum at 10 TeV does not significantly worsen the expected radiation damage.

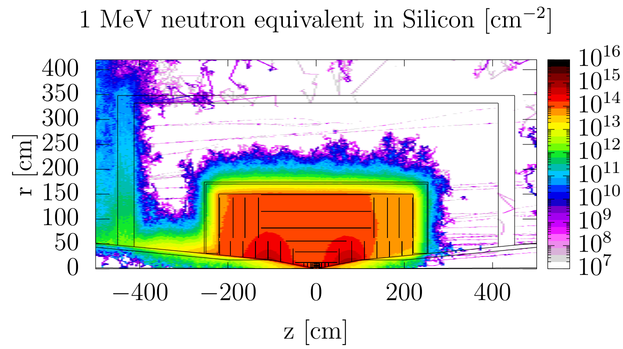

Figure 6: Radiation damage expressed in $\Phi_{n_{eq}}$ from a single μ beam going from left to right (per year of operation). In the most loaded region of the tracker, the 1 MeV-neutron equivalent fluence reaches values of $\sim 10^{15}$ cm^{-2}.

CONCLUSIONS

In this paper, we explored the decay-induced background in a 10 TeV muon collider. In particular, we assessed the dependency of the secondary particle fluence on the distance between IP and final focus magnets (L^*). The results showed only a moderate reduction of a few tens of percent when increasing L^* from 6 m to 10 m, at the expense of a more complex lattice design. In combination with our previous studies, which investigated the effect of dipolar field components in the final focus layout, we conclude that the lattice design offers a limited potential for mitigating the background. Another possibility for optimizing the physics performance at 10 TeV is the nozzle design. The simulations indicate that even a small modification of the nozzle tip affects the particle multiplicity around the IP. Since the most loaded tracker layers are placed in this region, a detailed investigation is required to minimize the background and the tracker occupancy. Finally, we provided a first estimation of the radiation damage in a generic 10 TeV detector (1 MeV neutron-equivalent fluence in silicon). The most loaded section is around the nozzle tip, due to the secondary neutrons leaking from the outer nozzle surface. The obtained radiation levels are considered acceptable for detector operation, but can be further reduced by modifying the borated polyethylene layer.

ISBN: 978-3-95450-231-8 ISSN: 2673-5490 doi: 10.18429/JACoW-IPAC2023-MOPA090

REFERENCES

[1] P. Bambade *et al.*, *The International Linear Collider: A Global Project*, 2019, doi:10.48550/ARXIV.1903.01629

[2] O. Brunner *et al.*, *The CLIC project*, 2022, doi:10.48550/ARXIV.2203.09186

[3] L. Evans and P. Bryant, "LHC Machine," *JINST*, vol. 3, no. 08, S08001, 2008, doi:10.1088/1748-0221/3/08/S08001

[4] H. A. Ali *et al.*, "The muon smasher's guide," *Rep. Prog. Phys.*, vol. 85, no. 8, p. 084 201, 2022, doi:10.1088/1361-6633/ac6678

[5] J. P. Delahaye *et al.*, *Muon colliders*, 2019, doi:10.48550/ARXIV.1901.06150

[6] N. V. Mokhov, Y. I. Alexahin, V. V. Kashikhin, S. I. Striganov, and A. V. Zlobin, "Muon Collider interaction region and machine-detector interface design," in *Proc. 2011 Particle Accelerator Conference, MOODN6, New York, NY, USA*, 2012, pp. 82–84.

[7] N. Mokhov and S. Striganov, "Detector backgrounds at muon colliders," *Phys. Procedia*, vol. 37, pp. 2015–2022, 2012, doi:10.1016/j.phpro.2012.03.761

[8] M. Palmer, "The US muon accelerator program," *arXiv preprint arXiv:1502.03454*, 2015.

[9] D. Schulte, "The International Muon Collider Collaboration," in *Proc. 12th International Particle Accelerator Conference (IPAC'21)*, Campinas, SP, Brazil, 2021, paper THPAB017, pp. 3792–3795, doi:10.18429/JACoW-IPAC2021-THPAB017

[10] G. Battistoni *et al.*, "Overview of the FLUKA code," *Annals of Nuclear Energy*, vol. 82, pp. 10–18, 2015, Joint International Conference on Supercomputing in Nuclear Applications and Monte Carlo 2013, SNA + MC 2013., doi:10.1016/j.anucene.2014.11.007

[11] C. Ahdida *et al.*, "New Capabilities of the FLUKA Multi-Purpose Code," *Front. Phys.*, vol. 9, p. 788 253, 2022, doi:10.3389/fphy.2021.788253

[12] *Fluka*, https://fluka.cern/.

[13] K. Skoufaris, C. Carli, and D. Schulte, "10 TeV Center of Mass Energy Muon Collider," in *Proc. 13th International Particle Accelerator Conference (IPAC'22)*, Bangkok, Thailand, 2022, paper MOPOTK031, pp. 515–518, doi:10.18429/JACoW-IPAC2022-MOPOTK031

[14] D. Calzolari and K. Skoufaris, "Machine-detector interface studies for a multi-TeV muon collider," *PoS*, vol. ICHEP2022, p. 063, 2022, doi:10.22323/1.414.0063

[15] F. Collamati *et al.*, "Advanced assessment of beam-induced background at a muon collider," *JINST*, vol. 16, no. 11, P11009, 2021, doi:10.1088/1748-0221/16/11/P11009

[16] CMS collaboration, "1-d plot covering cms tracker, showing fluka simulated 1 mev neutron equivalent in silicon including contributions from various particle types," CMS-DP-2015-022, Tech. Rep., 2015.